OPEN ACCESS

TamPub This document has been downloaded from TamPub.uta.fi
The Institutional Repository of University of Tampere

Japanese Journal of Applied Physics **57**, 117001 (2018)

REGULAR PAPER

https://doi.org/10.7567/JJAP.57.117001

Microelectrode array for noninvasive analysis of cardiomyocytes at the single-cell level

Tomi Ryynänen[1*†], Mari Pekkanen-Mattila[2†], Disheet Shah[2], Joose Kreutzer[1], Pasi Kallio[1], Jukka Lekkala[1], and Katriina Aalto-Setälä[2,3]

[1]*BioMediTech Institute and Faculty of Biomedical Sciences and Engineering, Tampere University of Technology, 33720 Tampere, Finland*
[2]*Heartgroup, BioMediTech Institute and Faculty of Medicine and Life Sciences, University of Tampere, 33520 Tampere, Finland*
[3]*Heart Center, Tampere University Hospital, 33520 Tampere, Finland*

*E-mail: tomi.ryynanen@tut.fi
†These authors contributed equally to this work.

Received July 9, 2018; accepted August 20, 2018; published online October 19, 2018

Microelectrode arrays (MEAs) are widely used to assess the electrophysiology of human pluripotent stem cell-derived cardiomyocytes (hPS-CMs). Traditionally, MEAs have been used to record data at the cell population level, but it would be beneficial to be able to analyze also at the single-cell level using MEAs. To realize this, we present a special MEA platform for recording field potential from single beating cardiomyocytes. The size and location of transparent indium tin oxide (ITO) electrodes have been optimized to make noninvasive studies of the electrophysiological activity of cardiomyocytes at the single-cell level possible and also to enable simultaneous video imaging through transparent electrodes and thus image-based analysis of the mechanical beating behavior of the same cardiomyocytes. Because of these characteristics, this novel platform provides a powerful tool for assessing the functionality of cardiomyocytes in basic cardiac research, disease modeling, as well as drug development and toxicology. © 2018 The Japan Society of Applied Physics

1. Introduction

Microelectrode arrays (MEAs) provide a valuable tool for studying the electrophysiology of cells. In addition, they provide a platform for long-term and on-line assessment of electrophysiological parameters at the baseline as well as during pharmacological or mechanical stress. MEAs have been widely used for assessing the electrical activity of multiple cell types, such as human stem cell-derived cardiomyocytes (hPS-CMs) and neurons at the cell population level.[1–4)]

Human induced pluripotent stem (iPS) cells are derived from somatic cells with a defined set of factors.[5)] They can be differentiated, e.g., into cardiomyocytes (CMs) by multiple methods, such as using defined growth factors or small molecules, or by co-culturing with mouse endodermal-like (END-2) cells.[6,7)] With the differentiation methods, all cardiac subtypes (pacemaker, atrial, and ventricular cells) can be produced and the differentiated hPS-CMs resemble the native human counterparts in their gene and protein expression as well as functional properties. Therefore, they are suitable for modeling human cardiomyocytes and use in studies of human heart development, cardiac function, and diseases as well as in drug development and toxicology, as reviewed earlier.[8)] hPS-CMs have been used in the evaluation of cardiac safety of new drug candidates especially for their effects on the field potential duration (FPD), which is analogous to the QT interval of electrocardiography (ECG).[9)]

The electrophysiological characteristics of single hPS-CMs can be assessed using the patch clamp technique and calcium (Ca^{2+})- and voltage-sensitive dyes. The patch clamp technique is a gold standard for the assessment of cardiomyocyte action potential. However, it is labor-intensive and has a low throughput and therefore not suitable for high-throughput-type early-stage drug screening studies. Ca^{2+}- and voltage-sensitive dyes are suitable for intermediate-throughput-type studies of cardiomyocyte electrophysiology at the single-cell and cell population levels and can be used in preclinical drug testing approaches. However, all these aforementioned methods are either invasive or toxic to the cells and thus, long-term experiments are not applicable.

MEAs have been a widely used for assessing electrical activity and signal propagation as well as the conduction velocity of hPS-CMs.[10–12)] hPS-CM measurements using conventional MEAs consisting of 30 μm electrodes and 200 μm pitch have been limited to cell clusters or monolayers; therefore, signals are gained from a cell population. However, similar to single-cell transcriptomic and proteomic studies, analyses of the electrophysiological characteristics using individual cells would produce a more accurate representation of the cells than bulk measurements.

There is no fundamental reason why conventional MEAs are not applicable to single-cell studies. However, owing to the relatively small electrode size, the noise level is high and the signal amplitude of a single cardiomyocyte is low. Thus, detecting signals from single cells by conventional MEAs is very challenging. An additional difficulty is getting the single cells on the electrodes in a conventional layout. Using conventional MEAs, we have not been able to detect signals from single cells, and to the best of our knowledge there have been no reports of studies of the electrical activity of single hPS-CMs using traditional MEAs. Because of these reasons, performing single-cell studies using conventional MEAs is not feasible; thus, the single-cell-optimized MEAs were produced.

By assessing the electrophysiology or calcium transients of cardiomyocytes, the cardiac function is only measured partly while ignoring the biomechanics of the actual contraction of the cardiomyocytes. Previously, the biomechanics of the cardiomyocyte contraction have been assessed in vitro by atomic force or traction force microscopy.[13,14)] However, recent video microscopy methods have proven to provide a

Content from this work may be used under the terms of the Creative Commons Attribution 4.0 license. Any further distribution of this work must maintain attribution to the author(s) and the title of the work, journal citation and DOI.

© 2018 The Japan Society of Applied Physics

relatively simple and noninvasive alternative to studying the biomechanics of cardiac contraction.[15–18] In a recent work, a video microscopy method was utilized, based on digital image correlation (DIC) and more specifically on its subtype, the minimum quadratic difference (MQD) method, which has been developed mainly for particle image velocimetry (PIV).[16] The video microscopy method quantifies the biomechanics, i.e., the movement of CMs in a noninvasive and label-free manner, enabling high-throughput-type screening, as well as long-term measurements.[15–17] Video analysis reveals information on the motion of CMs and, recently, video microscopy has also been combined with Ca^{2+} imaging.[19] By combining ionic and contraction data, a deeper understanding of the electromechanical coupling of cardiomyocyte contraction will be gained and new insights into cardiac diseases and drug effects may be revealed.

The aim of this study was to produce a MEA platform that contains electrodes that can measure the electrophysiological parameters of single hPS-CMs. The platform is designed for cell cultures where single hPS-CMs are plated on a MEA plate and only one cell is attached on the electrode. Owing the transparency of the electrodes, the platform also enables simultaneous measurement of the electrophysiological and biomechanical parameters of the contraction of single hPS-CM contraction noninvasively. The proposed platform consists of transparent electrodes, which are larger than those in conventional MEA platforms. In addition, the electrode layout is optimized for hPS-CMs. The custom-made MEA platforms are used with a conventional MEA amplifier, and the transparent electrodes enable simultaneous imaging and video analysis of the hPS-CMs. Therefore, the proposed approach provides data on both electrophysiological and biomechanical characteristics of a single cardiomyocyte, which will be utilized in studies of, e.g., iPS-based genetic cardiac disease modeling.

2. Materials and methods

2.1 MEA design, fabrication, and characterization

In measuring the field potential from a single cell with a MEA, there are two main challenges: how to 1) place a cell to be sufficiently close to the electrode and 2) optimize the signal-to-noise ratio by adjusting the size of the electrodes. If the electrode is much larger than the cell, the signal-to-noise ratio becomes small. However, too small electrodes possess a higher noise level by nature because impedance and noise are inversely dependent on the electrode area. For these reasons, the field potential signals of single cardiomyocytes are difficult to separate from noise. With the conventional MEAs having ~30-μm-diameter electrodes with ~200 μm spacing, it has been impossible to assess the electrical characteristics of hPS-CMs at the single-cell level.

The aim of this study was to design a MEA electrode layout that simultaneously increases the probability of cells to be located in optimal proximity to the electrodes and provides sufficient signal-to-noise ratio. In Layout 1, the cell culture area is covered by long and narrow electrodes resembling finger electrodes [Fig. 1(a)] to fulfill especially the first requirement for a design. For Layout 2 [Fig. 1(b)], we focus on evaluating different electrode sizes and shapes. The electrodes are circular or oval in shape, with some being split into halves or quarters. In this layout, the electrodes are located throughout the cell culture area. In Layout 3 [Figs. 1(c) and 1(d)], circular electrodes having a diameter of 80 μm are placed around the perimeter of the cell culture area. The center-to-center distance of the electrodes varies from 250 to 460 μm. Some of the electrodes have stripes or round holes to provide topography, which aims to orientate the cells or induce the cells to attach to the electrodes. Again, some of the electrodes are divided into separate halves as in Layout 2.

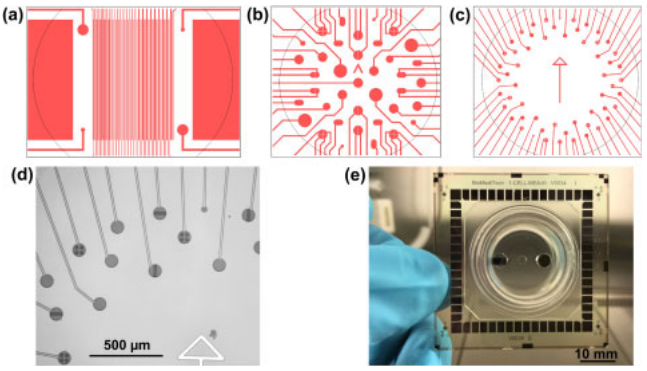

Fig. 1. (Color online) (a) Electrode Layout 1, (b) Layout 2, and (c) Layout 3. The black circles represent the central opening in the PDMS ring; diameters, 2 mm in Layouts 1 and 2, and 3.5 mm in Layout 3. (d) 5× microscopy image of Layout 3 MEA. (e) Specially designed PDMS ring on layout 3 ITO MEA. At the center there is an opening for microelectrodes and two bigger openings for ground electrodes. The right-angled ground electrode on the left was used in this study.

2.2 MEA fabrication

Figures 2(a)–2(k) show the fabrication process for Layout 3 in detail. The MEAs in Layouts 1 and 2 were fabricated using mostly the same process as that for MEAs in Layout 3. Two different versions of MEAs having Layout 3 were fabricated; one with opaque titanium (Ti) electrodes[20] and the other with transparent indium tin oxide (ITO) electrodes. The processing of MEAs with Ti electrodes started by e-beam deposition of 400 nm of Ti on $49 \times 49 \times 1\,mm^3$ soda lime glass substrates (Gerhard Menzel). Next, a positive photoresist (Futurrex PR1-2000A) was used as an etching mask in wet etching the MEA layout on the Ti layer. In the case of MEAs with ITO electrodes, a ~180 nm, 8–10 Ω/sq ITO layer was readily deposited on $49 \times 49 \times 0.7\,mm^3$ boro-aluminosilicate glass substrates (Universitywafer). In that case, the in-house process was started by lift-off patterning Ti alignment marks on the ITO-coated substrates. Next, a positive photoresist was used as an etching mask in etching the MEA layout on the ITO layer using argon in a reactive-ion etching (RIE) process. The remaining process steps were the same for the Ti and ITO versions. A 500 nm Si_3N_4 layer was deposited by plasma-enhanced chemical vapor deposition (PECVD) as the insulator layer and openings for electrodes and contact pads were dry-etched with a positive photoresist as an etching mask. Before 400 nm of titanium nitride was deposited by ion-beam-assisted e-beam deposition (IBAD),[21] to protect the contact pads, the electrode area was covered with a drop of photoresist. Finally, lift-off and resist removal were carried out using acetone in an ultrasound bath. Photolithography masks used in this work were fabricated in-house using a μPG501 maskless exposure system (MED; Heidelberg Instruments Mikrotechnik) on chrome mask blanks (Clean Surface Technology). In the case of Layout 1, part of the

© 2018 The Japan Society of Applied Physics

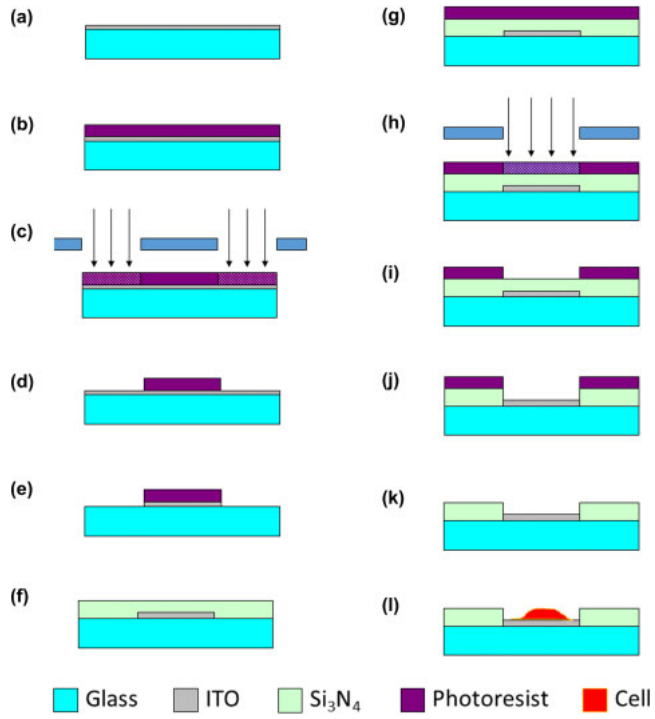

Fig. 2. (Color online) (a–k) MEA fabrication process. (a) Glass substrate coated with ITO or Ti, (b, g) spin coating with photoresist, (c, h) UV exposure of photoresist, (d, i) developed resist pattern, (e) electrode and track pattern dry etched to ITO or Ti, (f) PECVD of Si_3N_4, (j) dry etching openings for electrodes, and (k) removal of photoresist. Steps to fabricate alignment marks for ITO MEA and deposition of TiN to protect contact pads are excluded for simplicity. (l) Cardiac cell on MEA electrode. Owing to the edges formed by the Si_3N_4 insulator layer, the electrode is in a small pit, which may be favored by the cells. The dimensions in the drawing are not in scale.

exposures were, however, direct exposures using μPG501 instead of a mask aligner and the chrome masks.

2.3 MEA characterization

In order to characterize the impedance of the electrodes, a poly(dimethylsiloxane) (PDMS) ring was attached on top of the ready-made MEAs as a pool and was filled with Dulbecco's phosphate-buffered saline (PBS Dulbecco w/o Ca^{++}, Mg^{2+}, Biochrom) one day before the impedance measurements. The measurement system consisted of an Iviumstat potentiostat and multiplexers (Ivium Technologies), an MEA adapter (Multi Channel Systems MCS), and a Pt wire counter electrode (ALS-Japan). In addition, DRIREF-2 (World Precision Instruments) was used as the reference electrode for single-frequency measurements, where the impedance was measured at 1 kHz frequency. The result for both electrode types (ITO and Ti) is presented as the average of the median of 10 randomly selected nonpatterned electrodes from three MEAs. The impedance was characterized in more details for a randomly selected electrode over a frequency range from 1 to 100 000 kHz.

The simple PDMS rings used in the impedance measurements were removed and a specially designed PDMS ring was applied to the MEAs [Fig. 1(e)] providing small openings for the electrode area (2.0 mm in diameter for Layouts 1 and 2, and 3.5 mm in diameter for Layout 3) and for the ground electrodes (4 mm in diameter). The purpose of the PDMS ring is to restrict the cell culture area to enhance the cell attachment to the top of the electrodes and to prevent the cells from spreading out across the well, e.g., to the ground electrodes, where the beating of the cells would disturb the measurement by causing "reversed" signals to all of the electrodes. The silicone ring also provides a large reservoir for culture medium (1.5 ml). Silicone rings were fabricated as described previously.[22)]

Before plating hPS-CMs, the baseline noise was recorded in the cell culture medium consisting of KnockOut Dulbecco's modified Eagle's medium (KO-DMEM; Lonza), 20% fetal bovine serum (FBS; Lonza), 1% nonessential amino acids (NEAA; Cambrex), 2 mM Glutamax (Invitrogen), and 50 U/ml penicillin/streptomycin (Lonza) for 30 s with an MEA2100 MEA system (MCS). The average root mean square (RMS) noise level was calculated for each MEA and MEA type. Electrodes having an RMS noise level above 10 μV were considered faulty and were excluded from the calculations.

2.4 Cell culture and differentiation of hPS-derived cardiomyocytes

The human patient-specific iPSC line UTA.04602.WT was used in this study. The iPS cell line has been established from the fibroblasts of a healthy individual and cultured as described previously.[5,23)]

Differentiation of human pluripotent stem cells into cardiomyocytes was carried out via temporal modulation of canonical Wnt-signaling.[6)] The differentiated cells were dissociated into single cells with collagenase A (Roche Diagnostics).[7)] Single cells were suspended into the cell culture medium described above.

The MEA wells were first hydrophilized with FBS and then coated with 0.1% gelatin type A (Sigma-Aldrich). Immediately after coating, dissociated hPS-CMs were plated on each MEA by pipetting 50 μl of cell suspension consisting approximately 200–300 cells to the electrode area. The hPS-CMs were incubated in this volume of the medium for 1 h in an incubator to let the cells attach to the MEA. After incubation, the MEA was carefully filled with 1 ml of the cell culture medium described above. The medium was replaced with a fresh one for the MEAs every three days, and the MEAs were measured one day after the medium replacement.

2.5 Cell measurements and data analysis

Field potential (FP) was recorded 5–11 days after plating at 37 °C, and signals were recorded for 30 s. The sampling frequency was 20 kHz. Field potential was recorded during spontaneous baseline beating and after adding 50–100 nM E-4031 (Sigma-Aldrich) to the cell culture medium. The E-4031 solution was incubated 2 min before the measurements. The E-4031 solution was diluted and measurements performed in the cell culture medium as described above.

FP data were converted from the MCD format to Axon Binary File (ABF) using MC_DataTool software (MCS), and the ABF tile was converted to Axon Text File (ATF) using ClampFit version 10.3.0.2 (Molecular Devices). The FP signals in the ATF format were analyzed with an in-house-developed analysis module using Origin 2017 (Microcal OriginTM). Beating frequency by beats per minute (BPM), interbeat interval (IBI), and field potential duration (FPD) were extracted from the data. Bazett's formula was used to calculate the beat-rate-corrected FPD (cFPD).

The beating hPS-CMs on MEA chambers were imaged with a Zeiss Axio Observer-inverted phase contrast microscope and videos were taken with an Imperx Bobcat-camera

© 2018 The Japan Society of Applied Physics

and JAI-Tool software. Videos were recorded for 30 s at 60 frames per second using 20× magnification. Video and MEA recordings were taken manually at the same time; therefore, the recordings were not automatically synchronized in this study.

The recorded videos were analyzed with CellVisus software (BioMediTech), which uses the digital image correlation (DIC)-based analysis method as used previously for hPS-CMs.[16,24] From the videos, the average parameters of the biomechanics of the contraction were defined: (1) duration of contraction, (2) time when hPS-CMs contracted, (3) duration of relaxation, (4) incomplete relaxation time, and (5) time when the cells relaxed.

For immunocytochemical staining, the hPS-CMs on MEA chambers were fixed with 4% paraformaldehyde (PFA; Sigma-Aldrich). The hPS-CMs were stained with a goat anti-cardiac-troponin-T (anti-Tnt; 1:2000, Abcam) antibody and incubated at +4 °C overnight. Alexa Fluor 568-conjugated polyclonal IgG (Abcam) for the goat anti-Tnt antibody was used as the secondary antibody and incubated with the cells for 1 h at room temperature. Cells were mounted with Vectashield containing 4′,6-diamidino-2-phenylindole, difydrochloride (DAPI) for staining nuclei (Vector Labs Vectashield). Fluorescence was visualized using an Olympus IX51 phase contrast microscope equipped with fluorescence optics and recorded with an Olympus DP30BW camera. The images were processed with Image-J and Adobe Photoshop 7.0 software (Adobe Systems).

3. Results and discussion

3.1 MEA layout development and technical characterization

In Layout 1, the cells plated on the MEA attached to the electrodes with high probability as the finger-type electrodes filled most of the cell culture area. Unfortunately, the area where the hPS-CM crossed the electrode was very small compared with the total electrode size and the signal from the cell was overpowered by the noise. However, one cardiomyocyte was found to attach to a circular 100 µm electrode included for the process characterization reasons. From that electrode, we were able to measure the signal and obtain a preliminary proof that a single hPS-CM is measurable by the MEA if the electrode size is increased from the conventional size of 30 µm (data not shown).

With MEAs in Layout 2, cardiomyocyte signals were detectable from some of the electrodes. However, it was observed that a notable proportion of the plated hPS-CMs tended to attach to the edges of the cell culture area, near the PDMS ring. On the basis of this finding, all the electrodes in Layout 3 were placed on the outer perimeter of the cell culture area of the MEA in order to increase the probability of the cells to attach to the electrodes. With this approach, a larger number of electrodes provided a signal. Nevertheless, no significant differences between the electrodes with stripes or holes and the plain electrodes were observed.

The impedances of ITO and Ti electrodes in Layout 3 were approximately 250 and 190 kΩ, respectively. The average baseline RMS noise in contrast was the same (5.4 ± 0.9 µV) for both materials. The phase and the magnitude of the impedance of a randomly selected round ITO electrode in a Layout 3 MEA are shown in Fig. 3 as functions of frequency.

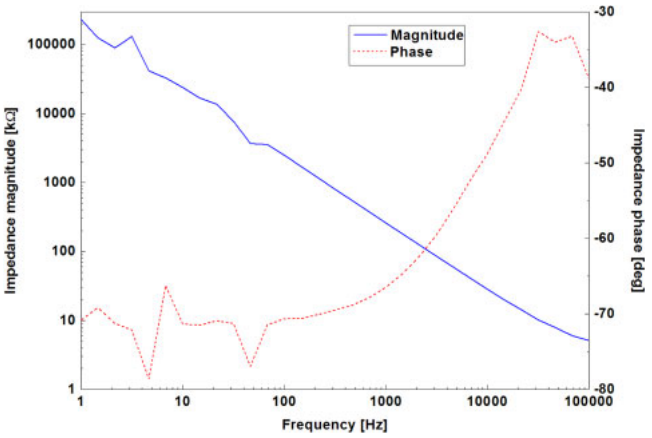

Fig. 3. (Color online) Phase and magnitude of impedance of a randomly selected round ITO electrode from a Layout 3 MEA as a function of frequency.

Compared with the standard 30 µm electrodes made of porous low-impedance materials such as titanium nitride (TiN) or platinum black, the impedances of our 80 µm ITO and Ti electrodes were 5–10 times higher despite their clearly larger sizes. Thus, one future development step in order to decrease impedance and noise level could be coating the Ti electrodes with TiN or with platinum black, as was done in a recent single-cell MEA approach in Ref. 29. These coatings, however, result in opaque electrodes. In contrast, decreasing the impedance of transparent ITO electrodes without losing their transparency is more challenging. Some improvement could be gained by increasing ITO thickness. However, because the impedance of the electrode–cell/medium interface dominates over track resistance, a more notable improvement requires new approaches, such as the development of new transparent electrode materials. Nevertheless, owing to the larger electrode size, the impedance was already 5–10 times smaller than the typical impedance of 30 µm electrodes made of ITO or Ti.[25] The baseline noise levels of both electrode types werethe same as those of commercial 30 µm TiN electrodes we previously measured for.[25] In addition to noise level and impedance, the material selection affects also the stimulation capability of the electrodes, which would enable, e.g., the pacing of hPS-CMs. That is however, left for future studies.

3.2 Cell attachment and measurements

The specific aim of this study was to grow no more than one hPS-CM on one electrode [Fig. 2(l)]. Therefore, the cell suspension was diluted and the total number of hPS-CMs plated on MEA plates was low, approximately 200–300 cells/well. The cells attached to the MEA plates during an overnight incubation and stayed attached as well as functional for at least two weeks on the MEA chambers. The hPS-CMs were beating and, therefore, functional when cultured in contact with the opaque Ti electrodes as well as transparent ITO electrodes.

The electrical activity of all the beating hPS-CMs attached to the top of the opaque and transparent electrodes in Layout 3 MEAs was detectable (4 MEA chambers used, 1–4 signals from each chamber observed). The signals were measured 5–11 days after the cell plating. The signal was very clear; therefore, the beating rate, beat-to-beat interval, and FP duration were measurable (Fig. 4, Table I). The signal character-

© 2018 The Japan Society of Applied Physics

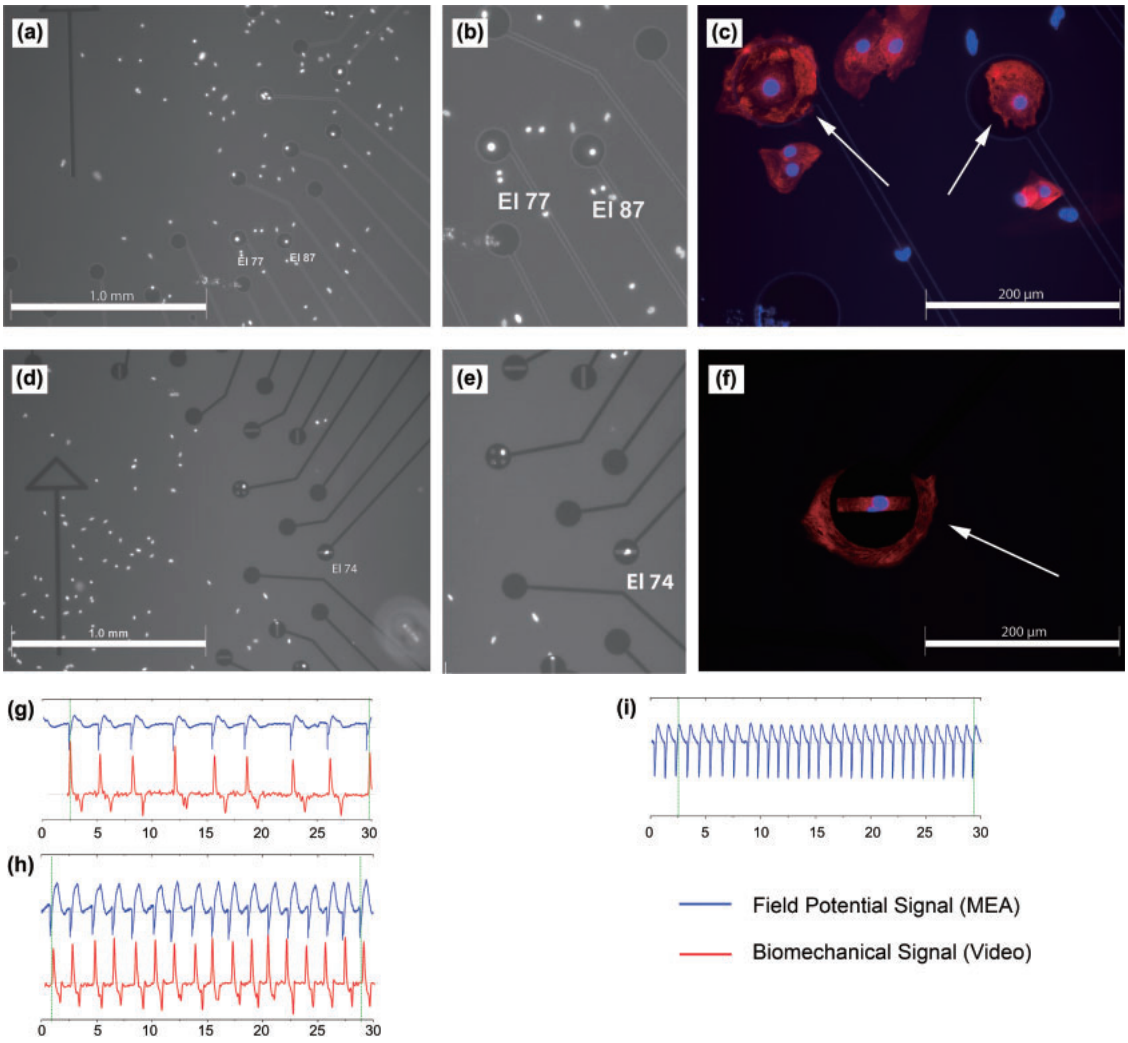

Fig. 4. (Color) (a–f) Immunocytochemical characterization of the cells plated on MEA chamber. (a) A MEA chamber with transparent electrodes and with DAPI staining indicating cell nuclei. (b) Insert in (a), indicating that both of the electrodes numbered 77 and 87 have one cell on each. (c) Immunocytochemical staining with cardiac-specific anti-troponin T antibody reveals that both of the cells on the electrodes are cardiomyocytes (indicated by arrows). (d) MEA chamber with opaque electrodes. (e) DAPI-stained nuclei are not visible on the electrodes with the inverted microscope if there are no holes on the electrode area, as on electrode 74. (f) Anti-troponin antibody staining shows that the cell on electrode 74 is a cardiomyocyte. (g–h) MEA signal (blue) aligned with the biomechanical signal of the contraction (red) analyzed by the video microscopy method from the hPS-CMs plated on the transparent electrodes. With both of the methods, a clear signal was obtained. (i) MEA signal gained from the hPS-CM on the opaque electrode.

Table I. Representative examples of the parameters describing the electrophysiology and biomechanics of the cardiac contraction of hPS-CM measured from the single hPS-CMs (Cells 1–6). The BPM and IBI gained from MEA and video data are comparable. With the single-cell MEA, the expected FPD prolonging effect of the the K^+-channel blocker E-4031 is observed. BPM, beats per minute; IBI, beat-to-beat interval; FPD, field potential duration; cFPD, corrected field potential duration.

		MEA data				Biomechanical (video) data		
		BPM	IBI (ms)	FPD B (ms)	cFPD B (ms)	BPM	IBI (ms)	Duration of mechanical activity (ms)
Cell 1	Baseline	38	1599	1055	834	38	1598	721
Cell 2	Baseline	17	3583	2623	1386	17	3461	1333
Cell 3	Baseline	93	644	480	598	94	639	164
Cell 4	Baseline	75	804	604	673	74	818	352
	E-4031	54	1112	829	786	N/A	N/A	N/A
Cell 5	Baseline	18	3426	1563	844	N/A	N/A	N/A
	E-4031	13	4508	1821	858	N/A	N/A	N/A
Cell 6	Baseline	62	965	702	714	N/A	N/A	N/A
	E-4031	48	1262	825	735	N/A	N/A	N/A

istics were comparable to those obtained from hPS-CM aggregates cultured using commercial MEA plates as reported previously.[16,23] In addition to the baseline data, the effects of the hERG-blocker E-4031 agent known to prolong the FPD interval were investigated. Prolongation of the FPD interval was detected at the single-cell level (Fig. 5 and Table I)

© 2018 The Japan Society of Applied Physics

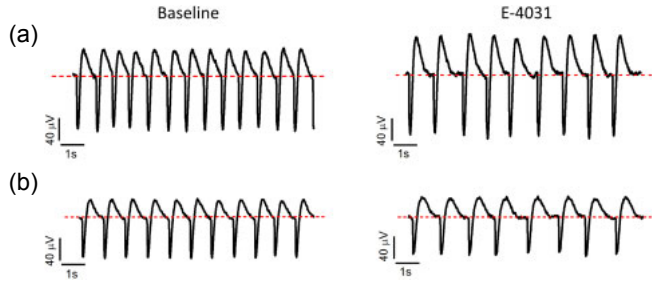

Fig. 5. (Color online) FP curves at the baseline and with E-4031 recorded from the hPS-CMs on the single-cell MEA. The FPD is prolonged owing to E-4031 as expected and this phenomenon is observed with the single-cell MEAs with transparent (a) as well as with opaque (b) electrodes.

demonstrating successfully the possibility of pharmaceutical testing on this novel single-cell MEA platform.

Owing to the transparency of the electrodes, the plated hPS-CMs could be imaged with the inverted phase contrast microscope. The videos of the hPS-CMs plated on the electrodes were analyzed by the Cell Visus software and the results of the analysis were comparable to the MEA data produced with the single-cell MEA system (Fig. 4, Table I, and video 1 in the online supplementary data at http://stacks.iop.org/JJAP/57/117001/mmedia). The obtained beating frequencies and beat-to-beat intervals were similar when recorded with the two methods.

The results showed that the MEA platform we developed can simultaneously record electrophysiological and biomechanical data and can thus be used for studies of cardiomyocyte function at the single-cell level owing to the transparency of the electrodes. Therefore, with this method, we can assess, e.g., the electromechanical coupling of hPS-CMs,[16] which provides a valuable tool for evaluating, for example, the proarrhythmic risk of novel drug candidates. However, the correlation between the electrical and mechanical functions of single hPS-CMs will be assessed in detail in future studies, since it is not within the scope of this study.

The beating was also observed from the opaque electrodes possessing gaps or holes (video 2 in the online supplementary data at http://stacks.iop.org/JJAP/57/117001/mmedia). However, video analysis was not possible and the contraction parameters could not be assessed. Therefore, to obtain both the MEA and video data, we concluded that the electrodes have to be transparent.

In this study, the entire cell culture area was coated with gelatin to support cell attachment. To increase the number of single cells attached on single electrodes, one possibility is the selective patterning of the electrodes with gelatin or other extracellular matrix proteins.[26] Recently, three-dimensional (3D) printing technologies have been applied to the generation of 3D cardiac patches composed of hPS-CMs and other supporting cell types with and without biomaterials.[27,28] Therefore, cell printing is an intriguing method that can be utilized also in the present single-cell MEA application, as the printer could print the cells exactly on the electrodes. Recently, Kaneko et al.[29] have proposed a MEA layout with small 8-μm-diameter and 1.4–3.0-μm-thick opaque platinum-black electrodes and agarose microchambers, where single CMs were seeded individually with a micropipette. With this method, the extracellular potential of a single CM was determined. However, the approach suffered from cell handling issues as well as difficulties with detecting two phases of FP peaks. We found the electrode diameter of 80 μm to be large enough to house a cell and to increase the probability of cell attachment compared with the standard 30 μm electrodes. Moreover, the diameter is sufficiently small to distinguish the cell signal from the background noise.

4. Conclusions

In this study, we introduced a MEA platform for assessing the electrophysiological characteristics (including FPD, beating frequency and beat-to-beat interval) of the hPS-CMs at the single-cell level. In addition, the transparency of the electrodes enables simultaneous video recording and analysis of the biomechanics of hPS-CM contraction and thus, enabling simultaneous electrophysiological and biomechanical characterization. With the video analysis, the durations of contraction and relaxation can be evaluated in addition to the alterations in the beating behavior such as a prolonged contraction or relaxation and oscillations in the beating.[16,24] The simultaneous electrophysiological and biomechanical characteristization provides a valuable tool for iPS-based disease modeling, as well as toxicology and drug development. In addition, the noninvasive nature of the novel platform enables the long-term assessment of the functionality of hPS-CMs at the baseline as well as the short- and long-term effects of alteration to putative drug agents. This platform opens up a new gateway to modeling cardiac diseases including genetic diseases and ischemia at the single-cell level.

Acknowledgments

This study was funded by Business Finland [formerly known as the Finnish Funding Agency for Technology and Innovation (TEKES)], the Council of Tampere Region, the Finnish Culture Foundation, and Päivikki and Sakari Sohlberg's foundation. We thank Antti Ahola for assistance with the video analysis and Haider Iftikhar for aid in ITO etching process development. We also acknowledge the Tampere Facility of Electrophysiological Measurements for their service.

1) T. J. Heikkilä, L. Ylä-Outinen, J. M. A. Tanskanen, R. S. Lappalainen, H. Skottman, R. Suuronen, J. E. Mikkonen, J. A. K. Hyttinen, and S. Narkilahti, Exp. Neurol. **218**, 109 (2009).
2) M. Pekkanen-Mattila, E. Kerkelä, J. M. A. Tanskanen, M. Pietilä, M. Pelto-Huikko, J. Hyttinen, H. Skottman, R. Suuronen, and K. Aalto-Setälä, Ann. Med. **41**, 360 (2009).
3) K. Asakura, S. Hayashi, A. Ojima, T. Taniguchi, N. Miyamoto, C. Nakamori, C. Nagasawa, T. Kitamura, T. Osada, Y. Honda, C. Kasai, H. Ando, Y. Kanda, Y. Sekino, and K. Sawada, J. Pharmacol. Toxicol. Methods **75**, 17 (2015).
4) L. Sala, D. Ward-van Oostwaard, L. G. J. Tertoolen, C. L. Mummery, and M. Bellin, J. Vis. Exp. **123**, e55587 (2017).
5) K. Takahashi, K. Tanabe, M. Ohnuki, M. Narita, T. Ichisaka, K. Tomoda, and S. Yamanaka, Cell **131**, 861 (2007).
6) X. Lian, C. Hsiao, G. Wilson, K. Zhu, L. B. Hazeltine, S. M. Azarin, K. K. Raval, J. Zhang, T. J. Kamp, and S. P. Palecek, Proc. Natl. Acad. Sci. U.S.A. **109**, E1848 (2012).
7) C. Mummery, D. Ward-van Oostwaard, P. Doevendans, R. Spijker, S. van den Brink, R. Hassink, M. van der Heyden, T. Opthof, M. Pera, A. B. de la Riviere, R. Passier, and L. Tertoolen, Circulation **107**, 2733 (2003).
8) Y. Yoshida and S. Yamanaka, Circ. Res. **120**, 1958 (2017).
9) M. Clements and N. Thomas, Toxicol. Sci. **140**, 445 (2014).

© 2018 The Japan Society of Applied Physics

10) J. Kuusela, V. J. Kujala, A. Kiviaho, M. Ojala, H. Swan, K. Kontula, and K. Aalto-Setälä, Springerplus **5**, 234 (2016).
11) J. Kuusela, J. Kim, E. Räsänen, and K. Aalto-Setälä, Stem Cell Rev. **12**, 698 (2016).
12) H. Zhu, K. S. Scharnhorst, A. Z. Stieg, J. K. Gimzewski, I. Minami, N. Nakatsuji, H. Nakano, and A. Nakano, Sci. Rep. **7**, 43210 (2017).
13) M. Pesl, J. Pribyl, I. Acimovic, A. Vilotic, S. Jelinkova, A. Salykin, A. Lacampagne, P. Dvorak, A. C. Meli, P. Skladal, and V. Rotrekl, Biosens. Bioelectron. **85**, 751 (2016).
14) M. C. Ribeiro, L. G. Tertoolen, J. A. Guadix, M. Bellin, G. Kosmidis, C. D'Aniello, J. Monshouwer-Kloots, M. J. Goumans, Y. Wang, A. W. Feinberg, C. L. Mummery, and R. Passier, Biomaterials **51**, 138 (2015).
15) H. Välimäki, J. Verho, J. Kreutzer, D. K. Rajan, T. Ryynänen, M. Pekkanen-Mattila, A. Ahola, K. Tappura, P. Kallio, and J. Lekkala, Sens. Actuators B **249**, 738 (2017).
16) A. Ahola, A. L. Kiviaho, K. Larsson, M. Honkanen, K. Aalto-Setälä, and J. Hyttinen, Biomed. Eng. Online **13**, 39 (2014).
17) L. Sala, B. J. van Meer, L. T. Tertoolen, J. Bakkers, M. Bellin, R. P. Davis, C. N. Denning, M. A. Dieben, T. Eschenhagen, E. Giacomelli, C. Grandela, A. Hansen, E. Holman, M. R. Jongbloed, S. M. Kamel, C. D. Koopman, Q. Lachaud, I. Mannhardt, M. P. Mol, D. Mosqueira, V. V. Orlova, R. Passier, M. C. Ribeiro, U. Saleem, G. Smith, F. L. L. Burton, and C. L. Mummery, Circ. Res. **122**, e5 (2018).
18) T. Hayakawa, T. Kunihiro, S. Dowaki, H. Uno, E. Matsui, M. Uchida, S. Kobayashi, A. Yasuda, T. Shimizu, and T. Okano, Tissue Eng. Part C **18**, 21 (2012).
19) A. Ahola, R. P. Pölönen, K. Aalto-Setälä, and J. Hyttinen, Ann. Biomed. Eng. **46**, 148 (2018).
20) T. Ryynänen, V. Kujala, L. Ylä-Outinen, I. Korhonen, J. M. A. Tanskanen, P. Kauppinen, K. Aalto-Setälä, J. Hyttinen, E. Kerkelä, S. Narkilahti, and J. Lekkala, Micromachines **2**, 394 (2011).
21) T. Ryynänen, M. Toivanen, S. Narkilahti, and J. Lekkala, Front. Neurosci. Conf. Abstr. MEA Meet. 2016/10th Int. Meet. Substrate-Integrated Electrode Arrays, 2016.
22) J. Kreutzer, L. Ylä-Outinen, P. Kärnä, T. Kaarela, J. Mikkonen, H. Skottman, S. Narkilahti, and P. Kallio, J. Bionic Eng. **9**, 1 (2012).
23) A. L. Lahti, V. J. Kujala, H. Chapman, A.-P. Koivisto, M. Pekkanen-Mattila, E. Kerkelä, J. Hyttinen, K. Kontula, H. Swan, B. R. Conklin, S. Yamanaka, O. Silvennoinen, and K. Aalto-Setälä, Dis. Model. Mech. **5**, 220 (2012).
24) A. L. Kiviaho, A. Ahola, K. Larsson, K. Penttinen, H. Swan, M. Pekkanen-Mattila, H. Venäläinen, K. Paavola, J. Hyttinen, and K. Aalto-Setälä, IJC Hear. Vasc. **8**, 19 (2015).
25) T. Ryynänen, L. Ylä-Outinen, S. Narkilahti, J. M. A. Tanskanen, J. Hyttinen, J. Hämäläinen, M. Leskelä, and J. Lekkala, J. Vac. Sci. Technol. A **30**, 041501 (2012).
26) L. Wang, L. Liu, X. Li, N. Magome, K. Agladze, and Y. Chen, Microelectron. Eng. **111**, 267 (2013).
27) L. Gao, M. Kupfer, J. Jung, L. Yang, P. Zhang, Y. Sie, Q. Tran, V. Ajeti, B. Freeman, V. Fast, P. Campagnola, B. Ogle, and J. Zhang, Circ. Res. **120**, 1318 (2017).
28) C. S. Ong, T. Fukunishi, H. Zhang, C. Y. Huang, A. Nashed, A. Blazeski, D. DiSilvestre, L. Vricella, J. Conte, L. Tung, G. F. Tomaselli, and N. Hibino, Sci. Rep. **7**, 4566 (2017).
29) T. Kaneko, H. Toriumi, J. Shimada, and F. Nomura, Jpn. J. Appl. Phys. **57**, 03EB03 (2018).

© 2018 The Japan Society of Applied Physics